

V.A. Romaka¹, Yu. Stadnyk², L. Romaka², V.V. Romaka³,
P. Demchenko², V. Pashkevich¹, A. Horyn²

Investigation of thermoelectric material based on Lu_{1-x}Zr_xNiSb solid solution. II. Modeling of characteristics

¹Lviv Polytechnic National University, S. Bandera Str. 12, 79013, Lviv, Ukraine
e-mail: volodymyr.romaka@gmail.com

²Ivan Franko L'viv National University, Kyryl & Mephody Str.6, 79005, L'viv, Ukraine
e-mail: lyubov.romaka@gmail.com

³Technische Universität Dresden, Bergstrasse 66, 01069 Dresden, Germany
e-mail: yromaka@gmail.com

The KKR (AkaiKKR software package) and FLAPW (Elk software package) methods were used to model the structural, thermodynamic, energetic, and electrokinetic characteristics of the Lu_{1-x}Zr_xNiSb semiconductor solid solution. It is shown that defects of acceptor nature are present in the structure of LuNiSb as a result of vacancies in positions 4a and 4c of Lu and Ni atoms, respectively, which generates two acceptor levels ε_A^{vac4a} and ε_A^{vac4c} in the band gap ε_g . When Zr atoms are introduced into the LuNiSb structure by replacing Lu atoms in position 4a, Zr atoms also occupy vacancies in this position, which increases the lattice parameter $a(x)$ and eliminates defects of acceptor nature and corresponding acceptor levels ε_A^{vac4a} . When the vacancies are filled, Lu atoms are displaced, which reduces the value of the unit cell parameter and generates defects of donor nature and donor levels ε_D^{4a} . The Ni atoms return to position 4c, which increases the $a(x)$ value and eliminates defects of acceptor nature and the corresponding acceptor levels ε_A^{vac4c} . At the lowest concentration of Zr atoms, the conduction type of Lu_{1-x}Zr_xNiSb changes from *p*- to *n*-type. The simulation results are consistent with experimental studies of Lu_{1-x}Zr_xNiSb.

Keywords: semiconductor, electrical conductivity, thermopower coefficient, Fermi level.

Received 17 December 2021; Accepted 26 July 2022.

Introduction

The study of Lu_{1-x}Zr_xNiSb semiconductive solid solution obtained by introducing Zr atoms into the LuNiSb structure by substituting of Lu atoms in the crystallographic position 4a revealed an unpredictable behavior of structural, energetic, and electrokinetic characteristics [1]. Since the atomic radius of Lu ($r_{Lu} = 0.173$ nm) is larger than Zr ($r_{Zr} = 0.160$ nm), we expected a monotonic decrease of the unit cell parameter values $a(x)$ of Lu_{1-x}Zr_xNiSb. In this case, structural defects

of donor nature should be generated in the Lu_{1-x}Zr_xNiSb semiconductor (Zr atom ($4d^25s^2$) has a greater number of *d*-electrons than Lu ($5d^16s^2$)). However, structural studies of Lu_{1-x}Zr_xNiSb showed an extremum on the dependence $a(x)$ at $x \approx 0.02$: in the concentration range $x = 0-0.02$, the $a(x)$ values increase rapidly, pass through the maximum and decrease rapidly at $x > 0.02$. Similar behavior of the lattice parameter $a(x)$ was observed for Er_{1-x}Zr_xNiSb solid solution [2, 3].

The nature of the change in the values of resistivity $\rho(T,x)$ and thermopower coefficient $\alpha(T,x)$ of Lu_{1-x}Zr_xNiSb

also turned out to be unexpected. At the lowest concentration of Zr atoms in the experiment ($x = 0.01$), the conductivity of $\text{Lu}_{1-x}\text{Zr}_x\text{NiSb}$ becomes metallic, and the negative values of the thermopower coefficient $\alpha(T, x)$ indicate the output of the Fermi level ε_F from the band gap ε_g to the conduction band ε_C . It turns out that at $x = 0$ we have a p -type of semiconductor when the Fermi level ε_F lies at a distance of ~ 10 meV from the top of the valence band ε_V , and at $x = 0.01$ it is located deep in the conduction band ε_C and electrons are the main carriers. Calculations show that if at position $4a$ the Lu atoms would be replaced by Zr atoms and donors were generated in $\text{Lu}_{1-x}\text{Zr}_x\text{NiSb}$, then at concentration $x \approx 0.02$ the Fermi level ε_F was near the middle of the band gap ε_g . And only at $x \geq 0.04$ it should cross the bottom of the conduction band ε_C , which would lead to metallization of electrical conductivity.

On the other hand, in the classical case of doping, for example, of a p -type semiconductor by a donor impurity, free electrons are first captured by acceptors (ionization of acceptors) to concentrations when the number of acceptors corresponds to the number of ionized donors. At higher concentrations, when all acceptors are ionized, the donor-supplied electrons become collectivized (free) and participate in the electrical conductivity. Thus, initially, the concentration of free holes decreases linearly to the number of introduced donors [4, 5]. In $\text{Lu}_{1-x}\text{Zr}_x\text{NiSb}$ this compensation mechanism is absent, but there is only a rapid increase in the number of electrons.

What caused this “non-classical” behavior of the electrokinetic characteristics of $\text{Lu}_{1-x}\text{Zr}_x\text{NiSb}$? Specifically, what structural changes in $\text{Lu}_{1-x}\text{Zr}_x\text{NiSb}$ caused such a significant restructuring of the semiconductor electronic system?

The answer to these questions lies in the plane of understanding the structural changes of the LuNiSb compound. Knowledge of the atomic distribution in the LuNiSb compound will allow us to understand the mechanism of introduction of Zr atoms into its structure during receipt of $\text{Lu}_{1-x}\text{Zr}_x\text{NiSb}$ solid solution and to predict the synthesis of thermoelectric materials with predetermined characteristics. For this purpose, the KKR (AkaiKKR software package) and FLAPW (Elk software package) methods were used to model the structural, thermodynamic, energetic, and electrokinetic

characteristics of $\text{Lu}_{1-x}\text{Zr}_x\text{NiSb}$ and compare them with the results of experimental studies.

I. Research methods

Calculations of the electronic structure, density distribution of electronic states (DOS), electron localization function (ELF), thermodynamic and electrokinetic characteristics, as well as optimization of the parameters of the crystal structure of $\text{Lu}_{1-x}\text{Zr}_x\text{NiSb}$ semiconductive solid solution, were performed using the method Korringa-Kohn-Rostoker (KKR) in the coherent potential approximation (CPA) and local density approximation (LDA), and also the full-potential method of linearized plane waves (FLAPW). KKR simulations were carried out using the AkaiKKR software package [6] in the local density approximation for the exchange-correlation potential with parameterization of Moruzzi, Janak, Williams (MJW) [7] in the semi-relativistic consideration of the core level and spin-orbit interaction. The Elk software package [8] was used for FLAPW calculations. The simulation was performed for a $10 \times 10 \times 10$ k -grid in both the local density (LDA) and generalized gradient (GGA) approximations. The Brillouin zone was divided into 1000 k -points, which were used to calculate the Bloch spectral function (band energy spectrum) and the density of electronic states. The width of the energy window was chosen to capture the semi-core states of p -elements. Visualization of volumetric data was carried out using the VESTA program [9]. The algorithm for modeling of the electronic structure was used according to the work [10]. Topological analysis and interpretation of DOS and ELF were performed within the framework of Bader’s theory [11].

II. Modeling of structural characteristics of $\text{Lu}_{1-x}\text{Zr}_x\text{NiSb}$

The results of calculation of the variation in the values of lattice parameter $a(x)$ of $\text{Lu}_{1-x}\text{Zr}_x\text{NiSb}$, $x = 0-1$, using both methods under the assumption that in the crystallographic position $4a$ Lu atoms are substituted by Zr atoms show a linear decrease of the lattice parameter (Fig. 1a). Such a decrease of the $a(x)$ values is predictable because the atomic radius of Zr is smaller than Lu one.

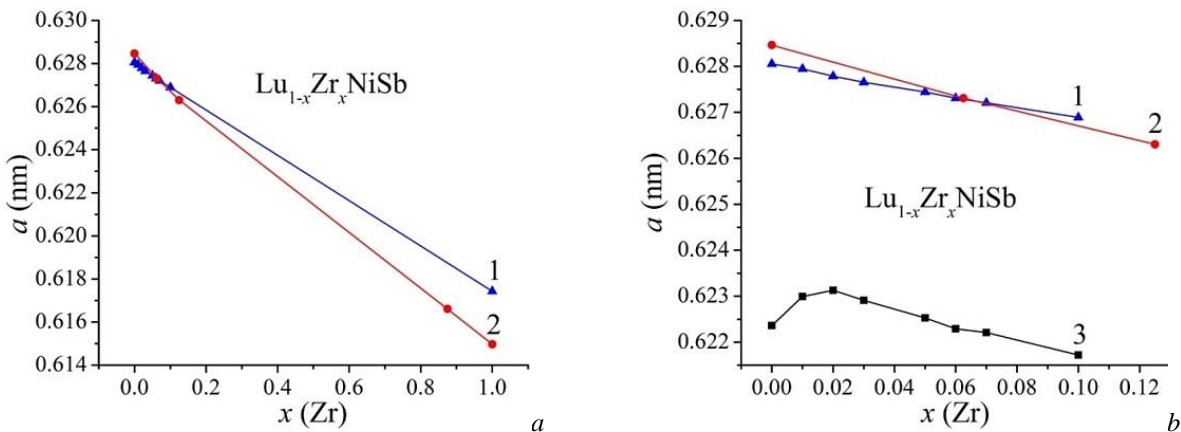


Fig. 1. Modeling of lattice parameter $a(x)$ of $\text{Lu}_{1-x}\text{Zr}_x\text{NiSb}$: $a - x=0-1.0$, $b - x=0-0.1$. 1 – AkaiKKR program, 2 – Elk program, 3 – experimental data.

From Fig. 1a, b, it is also seen that the lattice parameter values of the LuNiSb compound obtained by modeling the AkaiKKR software package [6] are smaller than when using the Elk software package [8].

At the same time, the simulation for the hypothetical ZrNiSb compound (another side of the $\text{Lu}_{1-x}\text{Zr}_x\text{NiSb}$ solid solution at $x = 1$) showed the opposite result: the lattice parameter values of the ZrNiSb compound obtained by AkaiKKR [6] are greater than those obtained by Elk [8]. Thus, the course of the $a(x)$ dependences of $\text{Lu}_{1-x}\text{Zr}_x\text{NiSb}$, obtained by different modeling methods, follows different laws (different angles of inclination of the rectilinear dependences $a(x)$). It's worth to remind that X-ray diffraction studies of $\text{Lu}_{1-x}\text{Zr}_x\text{NiSb}$ [1] revealed the nonmonotonic behavior of the $a(x)$ values of $\text{Lu}_{1-x}\text{Zr}_x\text{NiSb}$: at concentrations $x = 0-0.02$ the values $a(x)$ increase and at $x > 0.02$ decrease (Fig. 1b, dependence 3). It turned out that the angle of inclination of the $a(x)$ dependence of $\text{Lu}_{1-x}\text{Zr}_x\text{NiSb}$, obtained from the experiment at $x > 0.02$ coincides with that when using the software package Elk [8]. This result indicates a higher efficiency of the structural characteristics modeling of $\text{Lu}_{1-x}\text{Zr}_x\text{NiSb}$ by the FLAPW method compared with the KKR method.

Fact that $\text{Lu}_{1-x}\text{Zr}_x\text{NiSb}$ is characterized by nonmonotonic behaviour of lattice parameter values $a(x)$ (Fig. 1b) suggests that the Zr atoms introduced into the matrix of the half-Heusler phase LuNiSb not only replace the Lu atoms in position 4a, and also cause other structural changes. Let's analyze which ones.

Formally, based on geometric considerations, we can assume that the increase of the lattice parameter $a(x)$ of $\text{Lu}_{1-x}\text{Zr}_x\text{NiSb}$ could cause partial occupation of the crystallographic position 4c of Ni atoms by Zr atoms. After all, the atomic radius of the Ni atom ($r_{\text{Ni}} = 0.124$ nm) is the smallest among the components of $\text{Lu}_{1-x}\text{Zr}_x\text{NiSb}$ ($r_{\text{Sb}} = 0.159$ nm). However, such an assumption is unlikely due to the significant difference in the atomic radii of Zr and Ni. On the other hand, the authors [1, 3] suggested the existence of vacancies in the 4c position of Ni atoms. Therefore, there is a high probability of returning Ni atoms to position 4c (filling vacancies in position), which can lead to an increase of $a(x)$ values for $\text{Lu}_{1-x}\text{Zr}_x\text{NiSb}$. We also do not rule out the presence of vacancies in the 4a crystallographic position, which generates structural defects of acceptor nature. The occupation of these vacancies by impurity Zr atoms also generates the appearance of structural defects of donor nature and leads to an increase of $a(x)$ values of $\text{Lu}_{1-x}\text{Zr}_x\text{NiSb}$.

Thus, the results of modeling the variation of the lattice parameter values $a(x)$ of $\text{Lu}_{1-x}\text{Zr}_x\text{NiSb}$ and their comparison with the experimental results [1] suggest the following structural transformations:

- the presence of vacancies in the 4a position and the corresponding acceptor levels ε_A^{vac4a} in the band gap ε_g . The occupation of vacancies in the 4a position by Zr atoms leads to an increase of $a(x)$ values of $\text{Lu}_{1-x}\text{Zr}_x\text{NiSb}$, elimination of defects of acceptor nature, and corresponding acceptor levels ε_A^{vac4a} . In this case, the structural defects of donor nature are generated in the semiconductor, and the corresponding donor levels ε_D^{4a}

appear in the band gap ε_g .

- the return of Ni atoms to position 4c and the elimination of vacancies leads to an increase of $a(x)$ values of $\text{Lu}_{1-x}\text{Zr}_x\text{NiSb}$. At the same time, the corresponding acceptor levels ε_A^{vac4c} disappear in the band gap ε_g ;

- substitution of Lu atoms in the 4a position by Zr atoms leads to a decrease of the lattice parameter values $a(x)$ of $\text{Lu}_{1-x}\text{Zr}_x\text{NiSb}$ and generates structural defects of donor nature and the appearance of donor levels ε_D^{4a} in the band gap ε_g .

The following results of optimization of the crystal structure model for the LuNiSb compound based on the electronic spectrum calculation and its physical properties [3, 12] will show how the abovementioned considerations regarding the distribution of atoms in $\text{Lu}_{1-x}\text{Zr}_x\text{NiSb}$ correspond to the real state.

III. Modeling of thermodynamic characteristics of $\text{Lu}_{1-x}\text{Zr}_x\text{NiSb}$

Given that the ZrNiSb compound with the structure of MgAgAs does not exist [13], i.e. there is no 100% substitution of Lu atoms by Zr, it is important to establish the limits of the existence of $\text{Lu}_{1-x}\text{Zr}_x\text{NiSb}$ substitutional solid solution. For this purpose, in addition to X-ray structural studies, the simulation of thermodynamic characteristics for a hypothetical solid solution $\text{Lu}_{1-x}\text{Zr}_x\text{NiSb}$, $x = 0-1$, in the approximation of harmonic oscillations of atoms within the framework of the DFT density functional theory was performed. Variation of the values of the mixing enthalpy ΔH_{mix} (Fig. 2) for $\text{Lu}_{1-x}\text{Zr}_x\text{NiSb}$, $x = 0-1$, allows us to establish the existence range of the substitutional solid solution.

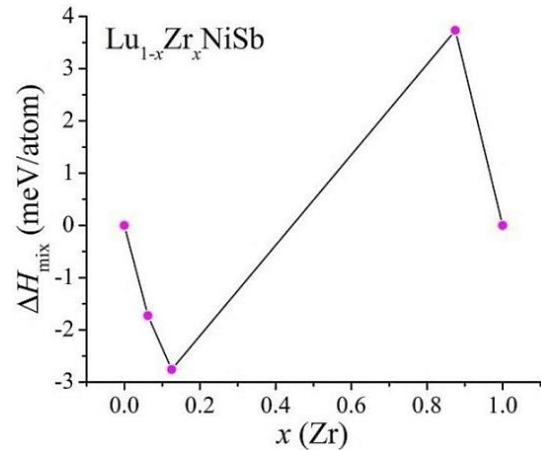


Fig. 2. Variation of mixing enthalpy values ΔH_{mix} of $\text{Lu}_{1-x}\text{Zr}_x\text{NiSb}$ calculated by Elk method.

At the concentration range $x \leq 0.125$, the values of the mixing enthalpy $\Delta H_{\text{mix}}(x)$ of $\text{Lu}_{1-x}\text{Zr}_x\text{NiSb}$ are negative and decrease, indicating the energy feasibility of substitution of Lu atoms by Zr. However, at higher concentrations of Zr atoms, $x > 0.125$, the dependence $\Delta H_{\text{mix}}(x)$ increases and changes sign at $x \approx 0.50$, which indicates the energy disadvantage of the formation of substitutional solid solution $\text{Lu}_{1-x}\text{Zr}_x\text{NiSb}$ at such concentrations. There is stratification (spinoidal decay of

phase), and the substitutional solid solution does not exist. Thus, the existence range of $\text{Lu}_{1-x}\text{Zr}_x\text{NiSb}$ solid solution is limited by the concentration $x \leq 0.125$, which includes the samples studied in [1].

IV. Modeling of electronic structure and refinement of crystal structure of LuNiSb compound

Modeling of the electronic structure of the LuNiSb compound for an ordered variant of the crystal structure with 100% occupancy by atoms of their own positions shows that the compound is a semiconductor with n -type of conductivity (Fig. 3). In this case, the Fermi level ε_F (dotted line) lies near the bottom of the conduction band ε_C , which in the experiment should give negative values of the thermopower coefficient $\alpha(T)$. However, this location of the Fermi level contradicts the results of experimental studies of the LuNiSb compound [1, 3, 12], which found that the compound is a p -type semiconductor, and the Fermi level ε_F lies near the top of the valence band at the distance of ~ 10 meV.

The discrepancy between the electronic structure of the LuNiSb compound, in particular the position of the Fermi level ε_F , obtained experimentally and by simulation, indicates the existence of defects in its crystal structure that generate energy levels of acceptor and donor nature in the band gap. Exactly the ratio of ionized acceptors and donors (the degree of semiconductor compensation [4]) determines the position of the Fermi level ε_F for LuNiSb. The fact that the Fermi level ε_F in LuNiSb lies near the valence band indicates the predominant number of acceptors over donors.

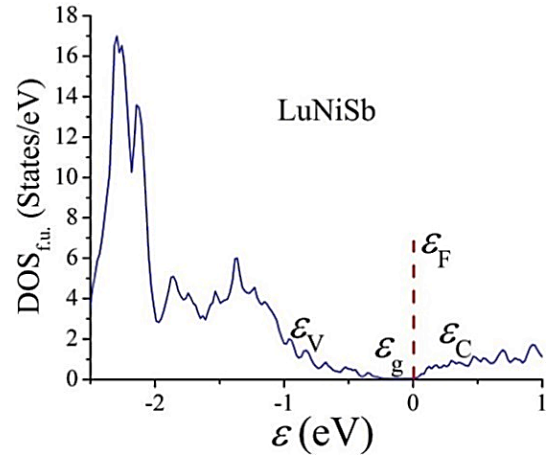


Fig. 3. DOS calculation of LuNiSb for ordered crystal structure with 100% occupancy of atoms of their own crystallographic positions.

During analysis of the crystal structure of LuNiSb, we assume the existence of vacancies in several crystallographic positions, which are the source of structural defects of acceptor nature. On the other hand, exactly the presence of vacancies will determine the ways of formation of structural defects and energy levels in the bandgap ε_g when impurity atoms are introduced into the structure of the LuNiSb compound. Therefore, it is important to establish the features of the crystal structure of the LuNiSb compound. Modeling of the electronic structure of the LuNiSb compound for different variants of the atoms distribution and the availability of vacancies was performed to refine its crystal structure as close as possible to the results of experimental measurements [1,

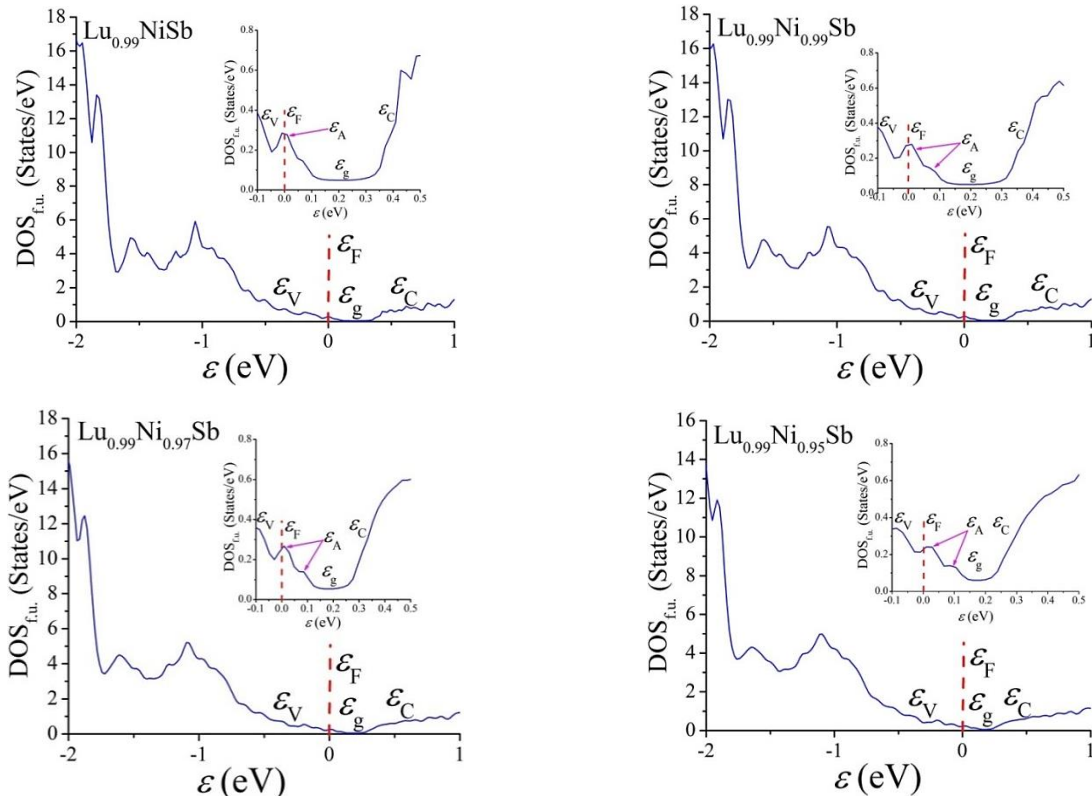


Fig. 4. Calculated DOS for LuNiSb with vacancies in positions 4a and 4c of Lu and Ni atoms, respectively.

3, 12]. The density distribution of electronic states DOS for the ordered model of the crystal structure of the LuNiSb compound is shown in Fig. 4. All atoms occupy their sites, but crystallographic position $4a$ is occupied by 99% Lu atoms and there are from 100% to 95% of Ni atoms in the $4c$ site. Unoccupied positions (vacancies) form structural defects of acceptor nature.

Thus, in the hypothetical compound $\text{Lu}_{0.99}\text{NiSb}$, the Fermi level ε_F rapidly changed its position and now lies at the edge of the valence band ε_V : the dielectric-metal conduction transition (Anderson transition) took place, and the holes are the main carriers. The location of the Fermi level ε_F at the edge of the valence band ε_V is clear because the absence of the Lu atom in $4a$ position generates a defect of acceptor nature and the corresponding acceptor level ε_A . Such a structural model of the compound in relation to the holes, as the main current carriers, corresponds to the experimental results [1, 3, 12]. However, experimental studies have established the semiconductor behavior of the resistivity $\ln(\rho(1/T))$ for LuNiSb with high- and low-temperature activation parts [14]. This means that in a real crystal, the Fermi level ε_F is located in the band gap ε_g of the semiconductor and not at the edge of the valence band ε_V , as shown by the simulation results for the case $\text{Lu}_{0.99}\text{NiSb}$.

If in the hypothetical $\text{Lu}_{0.99}\text{Ni}_{1-y}\text{Sb}$ compound vacancies will appear in the crystallographic position $4c$ of Ni atoms, then another acceptor level ε_A is generated in the $\text{Lu}_{0.99}\text{Ni}_{0.99}\text{Sb}$, $\text{Lu}_{0.99}\text{Ni}_{0.97}\text{Sb}$ and $\text{Lu}_{0.99}\text{Ni}_{0.95}\text{Sb}$ compounds (Fig. 4), and a rapid decrease of the values of the effective band gap ε_g with a velocity $\Delta\varepsilon_g/\Delta y=30$ meV/at.% was observed (Fig. 5). Here, the term “effective band gap ε_g ” means the energy gap between the “tails” of the continuous energy bands. The Fermi level ε_F is fixed by the acceptor level, which merges with the valence band ε_V . This location of the Fermi level ε_F does not agree with the experimental results, where it is located at a distance of ~ 10 meV from the top of the valence band ε_V .

It seems that the presence of 1% vacancies in the crystallographic position $4a$ of Lu atoms is too high, and, in the hypothetical compound $\text{Lu}_{0.99}\text{Ni}_{1-y}\text{Sb}$, we will not be able to observe in the experiment activation of holes from the Fermi level ε_F to the edge of the valence band ε_V .

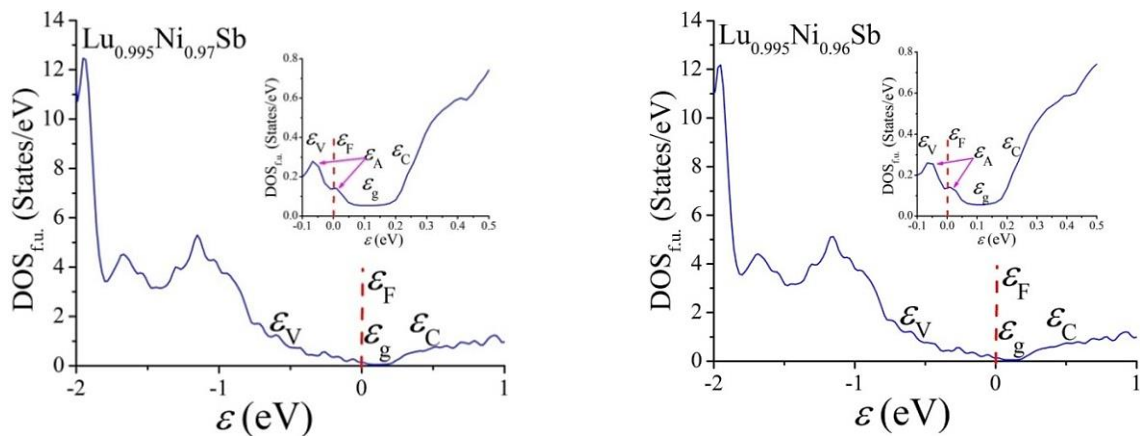


Fig. 6. Calculated DOS of $\text{Lu}_{0.995}\text{Ni}_{1-y}\text{Sb}$ with vacancies in positions $4a$ and $4c$ of Lu and Ni atoms, respectively.

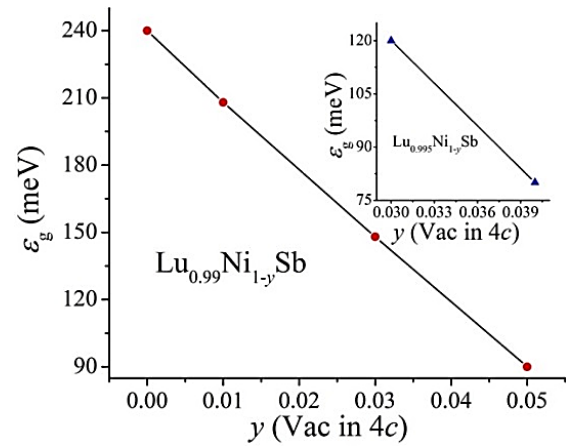


Fig. 5. Variation of effective band gap ε_g values in $\text{Lu}_{0.99}\text{Ni}_{1-y}\text{Sb}$ and $\text{Lu}_{0.995}\text{Ni}_{1-y}\text{Sb}$ (insert).

In the case of a smaller number of vacancies in $4a$ position of Lu atoms, for example, in the hypothetical compound $\text{Lu}_{0.995}\text{Ni}_{1-y}\text{Sb}$, two acceptor levels ε_A are also generated (Fig. 6), and the values of the effective band gap ε_g reduced with the velocity $\Delta\varepsilon_g/\Delta y=40$ meV/at.% (Fig. 5, insert). The model of the electronic structure of the hypothetical $\text{Lu}_{0.995}\text{Ni}_{1-y}\text{Sb}$ compound with vacancies in the crystallographic position $4c$ of Ni atoms assumes the location of the Fermi level ε_F at the edge of the valence band ε_V (Fig. 6). Formally, this model also does not agree with the results of the experiment. However, in the calculations, we neglect uncontrolled donors that are present in the crystal, and the position of the Fermi level ε_F is the result of compensation of ionized acceptors and donors. Therefore, we can assume that the model of the compound $\text{Lu}_{0.995}\text{Ni}_{0.97}\text{Sb}$ is close to the atomic distribution in a semiconductor.

V. Modeling of electrokinetic characteristics of $\text{Lu}_{1-x}\text{Zr}_x\text{NiSb}$

Modeling of the temperature dependences of the electrokinetic characteristics for the LuNiSb compound at temperatures of 4.2–70 K shows a rapid decrease in the resistivity values $\rho(T)$ in the range $T = 4.2\text{--}20$ K (Fig. 7). Such behavior $\rho(T)$ is characteristic of semiconductors when there is an increase of free current carriers number

due to their activation from the Fermi level ε_F to the continuous energy bands. In the case of the LuNiSb compound, such carriers are holes, which are indicated by positive values of the thermopower coefficient $\alpha(T)$, and this is consistent with the experimental results [1].

The introduction of Zr atoms into the structure of the LuNiSb compound by substituting Lu atoms at position 4a generates structural defects of donor nature in $\text{Lu}_{1-x}\text{Zr}_x\text{NiSb}$. Simulation of the variation of resistivity values $\rho(T,x)$ at the lowest concentration of Zr atoms ($x = 0.01$) shows two fundamentally different parts: at temperatures $T = 4.2\text{--}20$ K, the values $\rho(T,x)$ decrease, which is characteristic of semiconductors, and with increasing temperature they increase, indicating the metallic type of conduction (Fig. 7). In this case, the values of the thermopower coefficient of $\text{Lu}_{0.99}\text{Zr}_{0.01}\text{NiSb}$ rapidly decrease from the value of $\alpha_{4.2\text{K}}=225$ $\mu\text{V/K}$ to $\alpha_{70\text{K}} = -20$ $\mu\text{V/K}$. The change of the sign of the thermopower coefficient $\alpha(T)$ indicates a change in the type of conduction of the semiconductor when the main current carriers are electrons. In this case the Fermi level ε_F is located in the conduction band ε_C , which provides metallic conduction.

At an even higher concentration of Zr atoms ($x = 0.07$ and $x = 0.10$) in the temperature range $T = 4.2\text{--}70$ K, the sign of the thermopower coefficient $\alpha(T)$ remains negative, and the behavior of variation of the resistivity values $\rho(T,x)$ is similar to the case when the concentration of Zr atoms was $x = 0.01$ (Fig. 7).

The fact that the values of the resistivity $\rho(T, x)$ of $\text{Lu}_{1-x}\text{Zr}_x\text{NiSb}$ decrease at all concentrations of Zr atoms in the temperature range $T = 4.2\text{--}20$ K indicates that the donor states are deeply located in the band gap ε_g of the semiconductor. At low temperatures ($T < 20$ K), the thermal energy is insufficient for the activation of

electrons into the conduction band ε_C of $\text{Lu}_{1-x}\text{Zr}_x\text{NiSb}$. The fact that such band is a conduction band ε_C can be stated based on negative values of the thermopower coefficient $\alpha(T,x)$. However, at temperatures $T > 20$ K, thermal throwing of electrons from the donor level to the edge of the conduction band ε_C appear, accompanied by an increase of the free electrons concentration. In this case, the Fermi level ε_F enters into the conduction band ε_C : a dielectric-metal transition of the conduction (Anderson transition [4]) takes place. The character of the variation of the resistivity values $\rho(T,x)$ and the thermopower coefficient $\alpha(T,x)$ of $\text{Lu}_{1-x}\text{Zr}_x\text{NiSb}$ is unchanged at temperatures $T = 70\text{--}400$ K (Fig. 8).

Enlarging values of the resistivity $\rho(T,x)$ for $\text{Lu}_{1-x}\text{Zr}_x\text{NiSb}$ with increasing temperature is quite clear due to the presence of scattering mechanisms of current carriers in the semiconductor. High values of the thermopower coefficient $\alpha(T,x)$ in the temperature range $T = 70\text{--}400$ K show that $\text{Lu}_{1-x}\text{Zr}_x\text{NiSb}$ remains a highly doped semiconductor in which the Fermi level ε_F is located in the conduction band ε_C .

Thus, from the above can be mentioned the consistency of the experimental results [1] and calculated values of the electrokinetic characteristics of the semiconductive solid solution $\text{Lu}_{1-x}\text{Zr}_x\text{NiSb}$ (Figs. 7, 8). This is evidence of both the correctness of the experiment and the chosen method of modeling.

We can now answer the question of structural changes in $\text{Lu}_{1-x}\text{Zr}_x\text{NiSb}$, which caused a significant restructuring of the electronic system of the semiconductor, and consequently “nonclassical” behavior of its electrokinetic characteristics. The results of modeling the energy characteristic of LuNiSb compound suggest the presence of vacancies in positions 4a and 4c of Lu and Ni atoms,

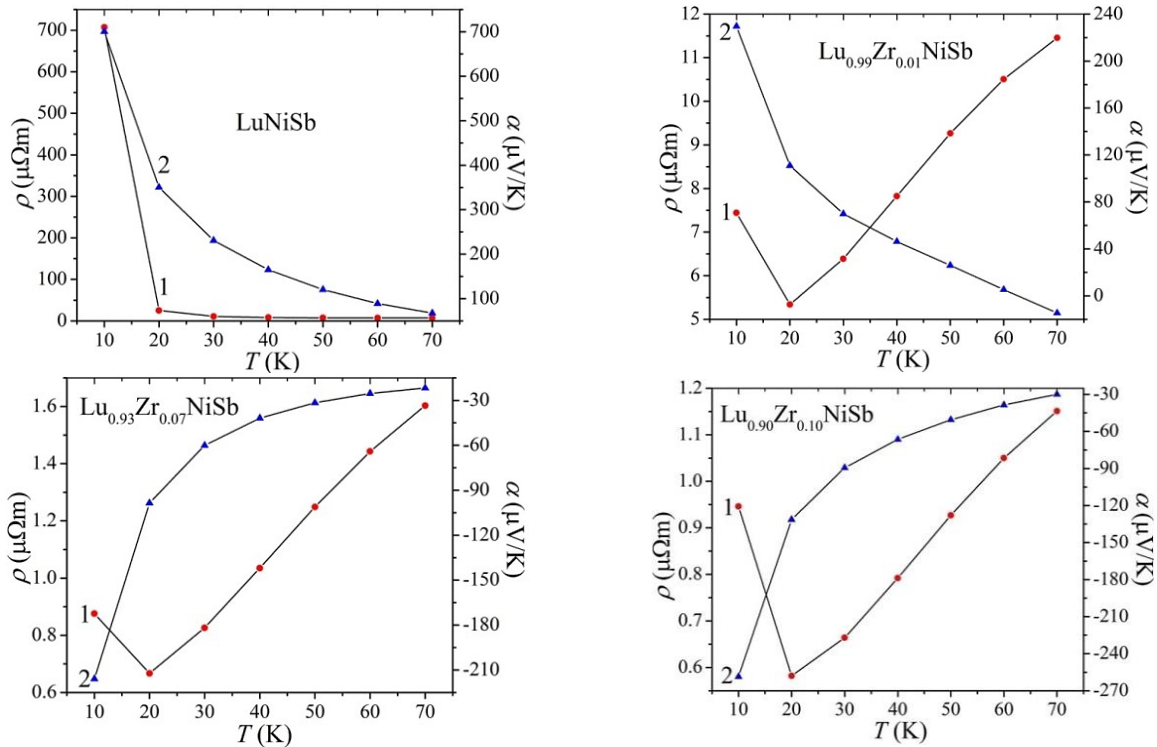


Fig. 7. Calculated variation of electrical resistivity $\rho(T,x)$ (1) and thermopower coefficient $\alpha(T,x)$ (2) for $\text{Lu}_{1-x}\text{Zr}_x\text{NiSb}$ at temperatures $T=4.2\text{--}70$ K.

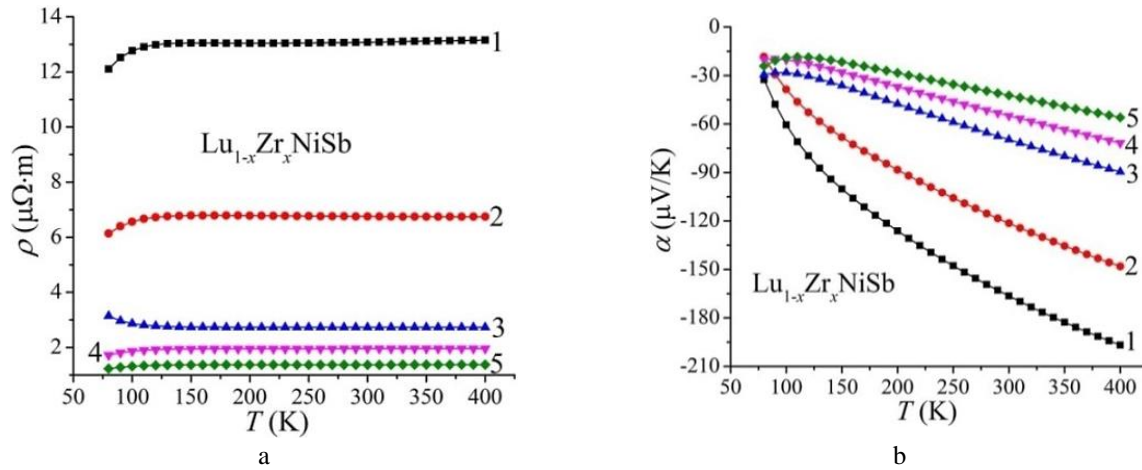


Fig. 8. Calculated electrical resistivity values $\rho(T,x)$ (a) and thermopower coefficient $\alpha(T,x)$ (b) of $\text{Lu}_{1-x}\text{Zr}_x\text{NiSb}$ at temperatures $T=70\text{--}400$ K: 1 – $x=0.01$; 2 – $x=0.02$; 3 – $x=0.05$; 4 – $x=0.07$; 5 – $x=0.1$.

respectively, which generates two acceptor levels $\varepsilon_A^{V_{ac4a}}$ and $\varepsilon_A^{V_{ac4c}}$ in the band gap ε_g . When Zr ($4d^25s^2$) atoms are introduced into the LuNiSb structure by replacing Lu ($5d^16s^2$) atoms in position $4a$, Zr atoms first occupy vacancies in this position, which leads to an increase of the unit cell parameter (Fig. 1b, dependence 3) and elimination of defects of acceptor nature and the corresponding acceptor levels $\varepsilon_A^{V_{ac4a}}$. At the same time, Ni atoms return to position $4c$, which increases the $a(x)$ value and eliminates defects of acceptor nature and the corresponding acceptor levels $\varepsilon_A^{V_{ac4c}}$. Exactly the elimination of vacancies, not their ionization during electron capture, is the fundamental feature that causes the “nonclassical” behavior of the electrokinetic characteristics of $\text{Lu}_{1-x}\text{Zr}_x\text{NiSb}$. When the vacancies are fully filled, Lu atoms are substituted, which reduces the value of the lattice parameter $a(x)$ and generates defects of donor nature and donor levels ε_D^{4a} .

Conclusions

A comprehensive study of the crystal and electronic structures, thermodynamic, electrokinetic, energetic properties of the thermoelectric material $\text{Lu}_{1-x}\text{Zr}_x\text{NiSb}$ allowed us to establish the nature of structural defects of donor and acceptor nature. It is shown that the structure of the basic compound LuNiSb has defects of acceptor nature

as a result of vacancies in the crystallographic positions $4a$ and $4c$ of Lu and Ni atoms, respectively, which generates acceptor levels in the band gap ε_g . Introduction of Zr impurity atoms into the structure of the LuNiSb compound by substitution of Lu atoms in position $4a$ generates structural defects of donor nature with simultaneous elimination of vacancies in positions $4a$ and $4c$ of Lu and Ni atoms (acceptor levels). The ratio of the concentrations of available donors and acceptors determines the location of the Fermi level ε_F and the conduction mechanisms of $\text{Lu}_{1-x}\text{Zr}_x\text{NiSb}$. The investigated solid solution $\text{Lu}_{1-x}\text{Zr}_x\text{NiSb}$ is a promising thermoelectric material.

Volodymyr Romaka – Professor of Lviv Polytechnic National University; volodymyr.romaka@gmail.com ;
Yuriy Stadnyk – Ph.D., Senior Scientist of Ivan Franko National University of Lviv, stadnykyu@gmail.com;
Lyubov Romaka – Ph.D., Senior Scientist of Ivan Franko National University of Lviv, lyubov.romaka@gmail.com;
Vitaliy Romaka – D.Sc., doctor of material science, Technische Universität Dresden, Dresden, Germany, vromaka@gmail.com;
Pavlo Demchenko – Ph.D., Senior Scientist of Ivan Franko National University of Lviv, pavlo.demchenko@lnu.edu.ua ;
Volodymyr Pashkevych – docent of National University “Lvivska Politechnika”, volodymyr.z.pashkevych@lpnu.ua;
Andriy Horyn – Ph.D., Senior Scientist of Ivan Franko National University of Lviv; andriy.horyn@lnu.edu.ua.

- [1] V.A. Romaka, Yu.V. Stadnyk, L.P. Romaka, A.M. Horyn, V.Z. Pashkevych, M.V. Rokomanuk, Materials XVII International Freik Conference on Physics and Technology of Thin Films and Nanosystems, Ivano-Frankivsk, October 11-16, 2021, P. 87.
- [2] V.A. Romaka, Yu. Stadnyk, L. Romaka, V. Krayovskyy, A. Horyn, P. Klyzub, V. Pashkevych, Phys. Chem. Sol. State 21, 689 (2020); <https://doi.org/10.15330/pcss.21.4.689-694>.
- [3] V.A. Romaka, Yu.V. Stadnyk, V.Ya. Krayovskyy, L.P. Romaka, O.P. Guk, V.V. Romaka, M.M. Mykyychuk, A.M. Horyn, The latest heat-sensitive materials and temperature transducers, Lviv Polytechnic Publishing House, Lviv (2020). ISBN 978-966-941-478-6. [in Ukrainian].
- [4] B. I. Shklovskii and A. L. Efros, Electronic Properties of Doped Semiconductors, Springer, NY (1984).
- [5] V.A. Romaka, D. Fruchart, V.V. Romaka, E.K. Hlil, Yu.V. Stadnyk, Yu.K. Gorenko and L.G. Akselrud, Semiconductors 43(1), 7 (2009); <https://doi.org/10.1134/S1063782609010035>.

- [6] H. Akai, J. Phys.: Condens. Matter. 1(43), 8045 (1989); <https://doi.org/10.1088/0953-8984/1/43/006>
- [7] V.L. Moruzzi, J.F. Janak, A.R. Williams, Calculated electronic properties of metals, Pergamon Press, NY (1978).
- [8] S.Y. Savrasov, Phys. Rev. B 54(23), 16470 (1996); <https://doi.org/10.1103/PhysRevB.54.16470>.
- [9] K. Momma, F. Izumi, J. Appl. Crystallogr. 41(3), 653 (2008); <https://doi.org/10.1107/S0021889808012016>.
- [10] V.P. Babak, V.V. Shchepetov, J. Friction and Wear 39, 38 (2018); <https://link.springer.com/article/10.3103/S1068366618010038>.
- [11] R.F.W. Bader, Atoms in Molecules: A Quantum Theory, Clarendon Press, Oxford (1994).
- [12] R.V. Skolozdra, A. Guzik, A.M. Goryn, J. Pierre, Acta Phys. Polonica A 92(2), 343 (1997).
- [13] L. Romaka, A. Tkachuk, Yu. Stadnyk, V.A. Romaka, J. Alloys Compd. 470, 233 (2009); <https://doi.org/10.1016/j.jallcom.2008.03.030>
- [14] V.V. Romaka, L. Romaka, A. Horyn, P. Rogl, Yu. Stadnyk, N. Melnychenko, M. Orlovskyy, V. Krayovskyy, J. Solid State Chem. 239, 145 (2016); <https://doi.org/10.1016/j.jssc.2016.04.029>.

В.А. Ромака¹, Ю. Стадник², Л. Ромака², В.В. Ромака³,
П. Демченко², В. Пашкевич¹, А. Горинь²

Дослідження термоелектричного матеріалу на основі твердого розчину

$\text{Lu}_{1-x}\text{Zr}_x\text{NiSb}$.

II. Моделювання характеристик

¹ Національний університет "Львівська політехніка", вул. С. Бандери, 12, Львів, 79013, Україна,
volodymyr.romaka@gmail.com

² Львівський національний університет ім. І. Франка, вул. Кирила і Мефодія, 6, Львів, 79005, Україна,
lyubov.romaka@gmail.com

³ Технічний університет м. Дрезден, Бергштрассе, 66, 01069, Дрезден, Німеччина, vromaka@gmail.com

Методами KKR (пакет програм AkaiKKR) та FLAPW (пакет програм Elk) проведено моделювання структурних, термодинамічних, енергетичних та кінетичних характеристик напівпровідникового твердого розчину $\text{Lu}_{1-x}\text{Zr}_x\text{NiSb}$. Показано, що у структурі сполуки LuNiSb присутні дефекти акцепторної природи як результат наявності вакансій у позиціях 4a та 4c атомів Lu та Ni відповідно, що генерує у забороненій зоні ϵ_g два акцепторні рівні ϵ_A^{Vac4a} та ϵ_A^{Vac4c} . При введенні до структури LuNiSb атомів Zr шляхом заміщення у позиції 4a атомів Lu відбувається зайняття атомами Zr вакансій у цій позиції, що збільшує період елементарної комірки $a(x)$ та ліквідує дефекти акцепторної природи і відповідні акцепторні рівні ϵ_A^{Vac4a} . За повного заповнення вакансій відбувається витіснення атомів Lu, що зменшує значення періоду комірки та генерує дефекти донорної природи і донорні рівні ϵ_D^{4a} . При цьому атоми Ni повертаються у позицію 4c, що збільшує значення $a(x)$ та ліквідує дефекти акцепторної природи і відповідні акцепторні рівні ϵ_A^{Vac4c} . За найменшої концентрації атомів Zr відбувається металізація та зміна типу провідності $\text{Lu}_{1-x}\text{Zr}_x\text{NiSb}$ з p- на n-тип. Результати моделювання узгоджуються з експериментальними дослідженнями $\text{Lu}_{1-x}\text{Zr}_x\text{NiSb}$.

Ключові слова: напівпровідник, електропровідність, коефіцієнт термо-ерс, рівень Фермі.